J. Trop. Plant Pests Dis.
Vol. 26, No. 2 September 2026
Pages: 390–404

ISSN: 1411-7525
E-ISSN: 2461-0399
DOI : 10.23960/j.hptt.226390-404

RESEARCH PAPER

Induced expression and functional role of heat shock protein 70 in *Pentalonia nigronervosa* (PnHsp 70) during banana bunchy top virus (BBTV) transmission

Indah Nuraini[1], Siti Subandiyah[1,2], & Alan Soffan[2]

Manuscript received: 3 October 2025. Revision accepted: 5 December 2025. Available online: 07 July 2026

ABSTRACT

Heat shock protein 70 (Hsp70) plays a critical role in cellular stress responses and virus–vector interactions; however, its diversity and function in *Pentalonia nigronervosa*, the sole vector of banana bunchy top virus (BBTV), remain poorly understood. This study aimed to identify, characterize, and evaluate the expression of Hsp70/Hsc70 genes in *P. nigronervosa* during BBTV acquisition. RNA-seq datasets from viruliferous and non-viruliferous *P. nigronervosa* (SRX6918251–SRX6918252) were assembled and annotated, resulting in the identification of seven PnHsp70 and three PnHsc70 genes, which were deposited in GenBank (MW456681–MW456690). Molecular characterization included subcellular localization prediction, physicochemical analysis, structural modeling, and phylogenetic analysis. Differentially expressed gene (DEG) analysis was validated by quantitative real-time PCR (qRT-PCR) using plant access period (PAP) assays (0, 1, 5, 10, and 20 hours) on BBTV-infected banana plants. PnHsp70 showed high sequence similarity to Hsp70 proteins from aphids, particularly *Myzus persicae* and *Acyrthosiphon pisum*. Structural analyses revealed conserved Hsp70 domains and molecular features, whereas phylogenetic analysis grouped PnHsp70 with other hemipteran Hsp70 homologs. DEG analysis identified PnHsp1, PnHsp2, and PnHsc1 as BBTV-responsive genes. qRT-PCR demonstrated that PnHsp70 expression increased following BBTV acquisition, with peak induction at 1 hour and renewed upregulation at 20 hours PAP. These results suggest that BBTV acquisition induces PnHsp70 expression and support its potential involvement in BBTV–vector interactions. This study provides the first comprehensive characterization of Hsp70/Hsc70 genes in *P. nigronervosa* and offers new molecular insights into BBTV transmission.

Keywords: BBTV, Hsp70, *Pentalonia nigronervosa*, qRT-PCR, RNA-seq, vector–virus interaction

INTRODUCTION

Heat shock proteins (Hsps) constitute a highly conserved superfamily of molecular chaperones essential for proteostasis and cellular stress adaptation. First identified in *Drosophila* as heat-induced gene products, Hsps are now known to be ubiquitous across prokaryotic and eukaryotic organisms. As molecular chaperones, they assist other proteins in folding, refolding, and preventing aggregation under adverse conditions, thereby enabling cells to overcome environmental stresses (Hu et al., 2022; Nakamoto et al., 2014; Hartl et al., 2011). Hsps also assist proteins in entering various degradation pathways such as the lysosomal, autophagic, and ubiquitin–proteasome pathways. In addition, Hsps facilitate the clearance of damaged proteins and improve cellular resistance to heat and other stresses, including anoxia, ischemia, exposure to heavy metal ions, ethanol, nicotine, surgical stress, and viral infection (Lang et al., 2021; Tower, 2011).

Heat shock proteins (Hsps) form a conserved superfamily classified by molecular weight and homology into major families such as HspH, HspC, HspA (Hsp70), DNAJ, HspB, and the chaperonins HspD/E and CCT/TRiC (Kampinga et al., 2009). Among them, Hsp70 is the most extensively studied because of its high conservation and its value as a molecular marker for evolutionary relationships across domains of life (Hartl et al., 2011). Hsp70 occurs in multiple isoforms with either inducible or constitutive expression and localizes to various cellular compartment (Kregel, 2002; Wang et al., 2019). Functionally, Hsp70 assists viral protein maturation and replication and coordinates virus–host physiological responses (Taguwa et al., 2015). Its involvement has been demonstrated in tomato yellow leaf curl virus (TYLCV) transmission by *Bemisia*

Corresponding author:
Alan Soffan (alan.soffan@ugm.ac.id)

[1]Genetic Engineering Laboratory, Center for Biotechnology Studies, Graduate School of Universitas Gadjah Mada, Yogyakarta, Indonesia 55281
[2]Department of Plant Protection, Faculty of Agriculture, Universitas Gadjah Mada, Yogyakarta, Indonesia 55281

tabaci (Götz et al., 2012; Pusag et al., 2012; Gorovits et al., 2013), flock house virus (FHV) replication (Weeks et al. 2010), and plant infections caused by cucumber necrosis virus (CNV) and rice stripe virus (RSV) (Jiang et al., 2014; Alam & Rochon, 2015).

Pentalonia nigronervosa is the sole vector of banana bunchy top virus (BBTV) (Qazi, 2016). In addition to banana, this aphid utilizes alternative host plants such as heliconia and rat taro, which can sustain aphid populations, facilitating the persistence and spread of BBTV even in the absence of banana plants (Arimbawa et al., 2022; Arsi et al., 2025). However, the role of Hsp70 in this vector–virus interaction remains unknown. The availability of viruliferous and non-viruliferous transcriptomes (SRX6918251–SRX6918252) (Subandiyah et al., 2020) enables testing of the hypothesis that BBTV exposure induces differential Hsp70 expression in *P. nigronervosa*.

In this study, we aimed to identify and characterize Hsp70 members of *P. nigronervosa* from the RNA-seq data of *P. nigronervosa* using RNA-seq data available in GenBank under accession numbers SRX6918251 and SRX6918252, followed by phylogenetic analysis of Hsp70 and Hsc70 together with their homologous sequences. The possible role of Hsp70 in *P. nigronervosa* was further validated through expression analysis under different acquisition access periods of *P. nigronervosa* on BBTV-infected banana plants using quantitative real-time polymerase chain reaction (qRT-PCR). This comprehensive investigation is expected to confirm the pivotal role of Hsp70 in the vector *P. nigronervosa*, thereby providing significant insights for BBTV management.

MATERIALS AND METHODS

Research Site. The research was conducted at the Laboratory of Genetic Engineering, Inter-University Center (PAU) and the Department of Plant Protection, Faculty of Agriculture, Universitas Gadjah Mada, Yogyakarta, Indonesia. The experimental phase was completed in 2020, with subsequent bioinformatic analyses completed in 2023.

***Pentalonia nigronervosa* Mass Rearing.** *Pentalonia nigronervosa* colonies were reared on taro (*Caladium bicolor*) and banana (*Musa acuminata*) under controlled conditions (25 ± 2 ºC, 70 ± 10% RH, and a 12:12 hours light:dark photoperiod) in an insect-proof growth chamber. BBTV-free and BBTV-infected banana plants served as hosts for non-viruliferous and viruliferous *P. nigronervosa* colonies, respectively. BBTV infection in banana plants was confirmed by PCR using BBTV-R primers (F: 5′-TTGAGAAACGAAAGGGRAGC-3′, and R: 5′-GGTGTGCGCCTGGGAAG-3′), which produce ~1.1 kb amplicons (Stainton et al., 2012). Approximately 200 third-instar nymphs collected from taro plants were transferred to BBTV-infected banana plants to establish viruliferous colonies. Viruliferous and non-viruliferous aphids were maintained in separate insect-proof cages to avoid cross-contamination, and their infection status was verified by PCR.

Total RNA Extraction and cDNA Synthesis. Total RNA was extracted from pooled samples of five adult *P. nigronervosa* individuals from both viruliferous and non-viruliferous colonies using the Total RNA Mini Kit (Tissue) (Geneaid, Taiwan), following the manufacturer's instructions. Prior to extraction, insects were homogenized using a sterile pestle. The extracted RNA was treated with DNase I (Thermo Scientific, USA) to eliminate genomic DNA contamination. RNA concentration and quality were assessed using a spectrophotometer (MaestroGen, Taiwan) by evaluating the A260/280 and A260/230 ratios, while RNA integrity was confirmed by electrophoresis on a 2% agarose gel. First-strand cDNA was synthesized from 1 µg of total RNA using the RevertAid First Strand cDNA Synthesis Kit (Thermo Scientific, USA) with oligo(dT) primers in a 25 µL reaction volume. The resulting cDNA was diluted to a working concentration of 100 ng/µL for qRT-PCR analysis. Three biological replicates were prepared for each treatment.

Annotation of *P. nigronervosa* Hsp70 and Primer Design. RNA-seq datasets of *P. nigronervosa* (accessions SRX6918251 and SRX6918252) were retrieved from GenBank as FASTQ files (Subandiyah et al., 2020). De novo transcriptome assembly was performed using Trinity to generate unigenes, followed by functional annotation against the NR database to identify candidate Hsp70 sequences. Unigene CL336. Contig1_All, designated as PnHsp70-1 (representing the unigene with the highest FPKM value), was selected for primer design.

Primers for PnHsp70 and the reference gene actin were designed using Primer3. The primer pairs were as follows: PnHsp70-F (5′-TTCTTCCACGGTAGGTCCAC-3′) and PnHsp70-R(5′-GGCCGACAGAGAAGAGTACG-3′), generating a 160 bp fragment; and PnActin-F (5′-CGGAATCATCACCAACTGGG-3′) and PnActin-R (5′-GATGGCAACATACATGGCGG-3′), generating a 190 bp fragment.

To ensure cDNA quality prior to downstream analyses, PCR validation was performed using both the PnHsp70 primers and the universal COI barcoding primers LCO1490 and HCO2198 (Folmer et al., 1994), which amplify a 710 bp mitochondrial fragment commonly used for specimen identification and template quality assessment. PCR reactions were carried out using GoTaq Green Master Mix (Promega), and the amplified products were visualized on 2% agarose gels to confirm specificity and integrity.

Molecular Characterization of PnHsp70 and PnHsc70. Identified unigenes encoding Hsp70 were used as queries to search for homologous sequences using the BLASTN program available on the NCBI website. Subsequently, each nucleotide sequence encoding the PnHsp70 family was translated into an amino acid sequence using the ExPASy Translate tool to obtain the open reading frame (ORF), which was then used as a query for BLASTP analysis.

Based on the BLAST results, the first hit of each protein sequence was used as the basis for classifying Hsp70 types. Seven and three genes encoding PnHsp70 and PnHsc70, respectively, were identified. Physicochemical properties were analyzed using the ProtParam web server available on ExPASy. The CYS_REC web server was used to predict the presence of cysteine residues and their binding patterns.

Phylogenetic tree construction was performed by comparing PnHsp70 and PnHsc70 with homologous Hsp70 sequences from insect species belonging to other orders identified through BLASTP analysis. Query and homologous sequences were compiled using BioEdit (Hall, 1999) and aligned using ClustalX (Thompson et al., 1997). Phylogenetic trees were constructed using MEGA X software (Tamura et al., 2013) based on the neighbor-joining (NJ) method with the Poisson correction model, pairwise deletion, and 1000 bootstrap replications.

Protein structure, ligand-binding sites, and active sites were analyzed using the I-TASSER web server (Yang & Zhang, 2015) and SWISS-MODEL. Construction and visualization of protein secondary structures were carried out using Chimera 1.15rc and Discovery Studio 2020 Client. Subcellular localization was predicted using LocTree3. Three conserved Hsp70 signature motifs, namely IDLGTTYS, IFDLGGGTFDVSIL, and IVLVGGSTRIPKVQR/N/S, were identified according to Gupta & Singh (1994).

Differentially Expressed Genes (DEGs) and qRT-PCR Validation. Differentially expressed genes (DEGs) between viruliferous and non-viruliferous *P. nigronervosa* from RNA-seq datasets (SRX6918251 and SRX6918252) were analyzed using Bowtie2 for read alignment and RSEM for expression quantification, expressed as fragments per kilobase of transcript per million mapped reads (FPKM). DEGs were identified based on fold-change and statistical thresholds, and candidate PnHsp70 genes showing significant differential expression were selected for further validation by qRT-PCR.

qRT-PCR assays were conducted across four plant access periods (PAPs: 1, 5, 10, and 20 hours). Prior to treatment, *P. nigronervosa* colonies were maintained on taro, a non-host of BBTV, to ensure that aphids were BBTV-free. For each PAP, three biological replicates were collected, each consisting of 10 aphids, along with a control group (0 h PAP on BBTV-infected banana plants). All samples were preserved in RNAlater (Ambion) prior to RNA extraction.

Total RNA extraction and cDNA synthesis were performed as described above. PnHsp70 expression levels were quantified by qRT-PCR using PowerUp™ SYBR™ Green Master Mix (Thermo Fisher Scientific) on a Bio-Rad T100 system. The qRT-PCR cycling conditions followed the manufacturer's recommended protocol.

Data Analysis. qRT-PCR data were analyzed using the 2^−ΔΔCt method (Livak & Schmittgen, 2001). Relative expression levels of PnHsp70 were normalized against the reference gene PnActin. One-way analysis of variance (ANOVA) was used to determine significant differences in PnHsp70 expression among different plant access periods (PAPs), followed by Tukey's post hoc test. Statistical analyses were performed using SPSS version 16.0 software.

RESULTS AND DISCUSSION

Annotation of *P. nigronervosa* Hsp70 and Hsc70 Genes. Assembly and annotation of SRX6918251 and SRX6918252 resulted in the identification of seven Hsp70 and three Hsc70 genes, all of which were submitted to GenBank under the following accession numbers: PnHsp1 (GenBank: MW456685), PnHsp2 (MW456686), PnHsp3 (MW456681), PnHsp4 (MW456682), PnHsp5 (MW456683), PnHsp6 (MW456684), and PnHsp7 (MW456687), which belong to the Hsp70 group, whereas PnHsc1 (MW456688), PnHsc2 (MW456689), and PnHsc3 (MW456690) belong to the Hsc70 group (Supplementary Table 1).

Table 1. Hsp70 and Hsc70 diversity in *P. nigronervosa* based on Denovo transcriptome on Sequence Read Archive (SRA:SRX6918251 and SRX6918252) and their homologous sequences from GenBank

Name (Access code)	Nucleotide length	ORF length	Location	Data base	First hit homologous protein
PnHsp1 (MW456685)	2712	640		Nr	heat shock protein 70 A1-like [*Myzus persicae*] (XP_022167905.1)
				Nt	PREDICTED: *Myzus persicae* heat shock protein 70 A1-like (LOC111032040), mRNA (XM_022312213.1)
				Nr	heat shock protein 70 A1-like [*Acyrthosiphon pisum*] (XP_001945786.2)
PnHsp2 (MW456686)	2620	637		Nt	PREDICTED: *Myzus persicae* heat shock protein 70 A1-like (LOC111042433), mRNA (XM_022327049.1)
				Nr	heat shock protein 70 A1-like [*Acyrthosiphon pisum*] (XP_001945786.2)
PnHsp3 (MW456681)	1228	322		Nt	PREDICTED: *Acyrthosiphon pisum* heat shock protein 70 A1-like (LOC100160289), mRNA (XM_001945751.4)
				Nr	heat shock protein 70 B2 [*Acyrthosiphon pisum*] (XP_001949837.1)
PnHsp4 (MW456682)	3138	537		Nt	PREDICTED: *Myzus persicae* heat shock protein 70 B2-like (LOC111027111), mRNA (XM_022305334.1)
			Cytoplasm	Nr	heat shock protein 70 A1-like [*Acyrthosiphon pisum*] (XP_001945786.2)
PnHsp5 (MW456683)	1551	429		Nt	PREDICTED: *Acyrthosiphon pisum* heat shock protein 70 A1-like (LOC100160289), mRNA (XM_001945751.4)
				Nr	heat shock 70 kDa protein 14-like [*Myzus persicae*] (XP_022163794.1)
PnHsp6 (MW456684)	1686	497		Nt	PREDICTED: *Acyrthosiphon pisum* heat shock 70 kDa protein 14 (LOC100161502), mRNA (XM_001945733.4)
				Nr	heat shock 70 kDa protein 12A-like isoform X1 [*Acyrthosiphon pisum*] (XP_001951229.2)
Pnhsp7 (MW456687	2824	790		Nt	PREDICTED: *Acyrthosiphon pisum* heat shock 70 kDa protein 12A-like (LOC100167220), transcript variant X1, mRNA (XM_001951194.4)
PnHsc1 (MW456688)	3406	654		Nr	heat shock 70 kDa protein cognate 4 [*Acyrthosiphon pisum*] (XP_001951207.1)
				Nt	PREDICTED: *Acyrthosiphon pisum* heat shock 70 kDa protein cognate 4 (LOC100159065), mRNA (XM_001951172.4)
PnHsc2 (MW456689)	2646	679	Mitochondria	Nr	heat shock 70 kDa protein cognate 5 [*Rhopalosiphum padi*] (ASU92323.1)

Table 1. Continued. Hsp70 and Hsc70 diversity in *P. nigronervosa* based on Denovo transcriptome on Sequence Read Archive (SRA:SRX6918251 and SRX6918252) and their homologous sequences from GenBank

Name (Access code)	Nucleotide length	ORF length	Location	Data base	First hit homologous protein
				Nt	PREDICTED: *Myzus persicae* stress-70 protein, mitochondrial (LOC111031704), mRNA (XM_022311757.1)
PnHsc3 (MW456690)	2961	662	RE	Nr	PREDICTED: heat shock 70 kDa protein cognate 3 [*Diuraphis noxia*] (XP_015371071.1)
				Nt	*Acyrthosiphon pisum* heat shock protein cognate 3 (Hsc70-3), mRNA (NM_001162948.1)

The predicted amino acid sequences were subsequently used to search for homologous proteins by submitting the FASTA-formatted sequences to the BLASTP database.

PnHsp1, PnHsp2, PnHsp7, PnHsc1, PnHsc2, and PnHsc3 represented complete coding sequences (CDSs) with nucleotide lengths of 2712, 2620, 2824, 3406, 2646, and 2961 bp, encoding ORFs of 640, 637, 790, 654, 679, and 662 amino acids, respectively. In contrast, PnHsp3, PnHsp4, PnHsp5, and PnHsp6 were partial CDSs. BLAST results from both the nucleotide (Nt) and protein (Nr) databases revealed high similarity between PnHsp70 sequences and Hsp70 proteins from *Myzus persicae* and *Acyrthosiphon pisum*. Likewise, the closest homologs for PnHsc70 proteins were *Acyrthosiphon pisum* (Nr and Nt), *Rhopalosiphum padi* (Nr) and *Myzus persicae* (Nt), as well as *Diuraphis noxia* (Nr) and *Acyrthosiphon pisum* (Nt) for PnHsc1, PnHsc2, and PnHsc3, respectively.

Molecular characterization of PnHsp70 and PnHsc70. To better understand the characteristics of Hsp70 and Hsc70 in *P. nigronervosa*, several in silico analyses were performed using available web-based bioinformatics tools. PnHsp1 and PnHsc1 were selected for detailed characterization because DEG analysis revealed that these two proteins exhibited the highest FPKM values and represented complete CDSs.

Subcellular localization analysis using the LocTree3 web server indicated that all PnHsp70 proteins were localized in the cytoplasm. In contrast, PnHsc70 proteins were predicted to localize in different cellular compartments, namely the cytoplasm, mitochondria, and endoplasmic reticulum for PnHsc1, PnHsc2, and PnHsc3, respectively. Physicochemical characterization using the ProtParam server revealed that PnHsp70 and PnHsc70 contained 640 and 654 amino acid residues, with molecular weights of 69,964.98 and 71,386.68 Da and theoretical isoelectric points (pI) of 5.44 and 5.34, respectively. Both proteins contained 94 negatively charged residues and 81 positively charged residues.

The predicted extinction coefficients (ECs) of PnHsp70 and PnHsc70 were 34,880 and 33,600 $M^{-1}cm^{-1}$ respectively, assuming all cysteine residues formed cystines, and 34,380 and 33,350 $M^{-1}cm^{-1}$, respectively, assuming all cysteine residues were reduced. The instability indices of PnHsp70 and PnHsc70 were 33.66 and 35.95, respectively, indicating that both proteins are stable because the instability index values were below 40 (Guruprasad et al., 1990). The aliphatic indices of PnHsp70 and PnHsc70 were 82.02 and 79.22, respectively, suggesting that both proteins are stable across a broad temperature range (Ikai, 1980).

Both proteins possessed methionine (Met) at the N-terminus and were predicted to have half-lives of 30 hours in mammalian reticulocytes (in vitro), >20 hours in yeast (in vivo), and >10 hours in *Escherichia coli* (in vivo). The grand average of hydropathicity (GRAVY) values for PnHsp70 and PnHsc70 were −0.400 and −0.447, respectively, indicating hydrophilic or water-soluble properties (Kyte & Doolittle, 1982; Chang & Yang, 2013). The most abundant amino acids in PnHsp70 and PnHsc70 were alanine (9.7% and 8.3%), glycine (7.5% and 8.9%), and lysine (7.2% and 8.3%) (Figure 1).

Analysis of cysteine residues and disulfide bond patterns using the CYS_REC web server identified eight and four cysteine residues in PnHsp70 and PnHsc70, respectively (Table 2). However, no disulfide bonds were predicted among these residues. Disulfide bonds formed between cysteine residues are important for stabilizing molecular architecture and supporting biological functions (Wiedemann et al., 2020).

Multiple sequence alignment of PnHsp70 and PnHsc70 amino acid sequences using BioEdit and ClustalW identified three highly conserved Hsp70 family signature motifs (Figure 2): (1) IDLGTTYS

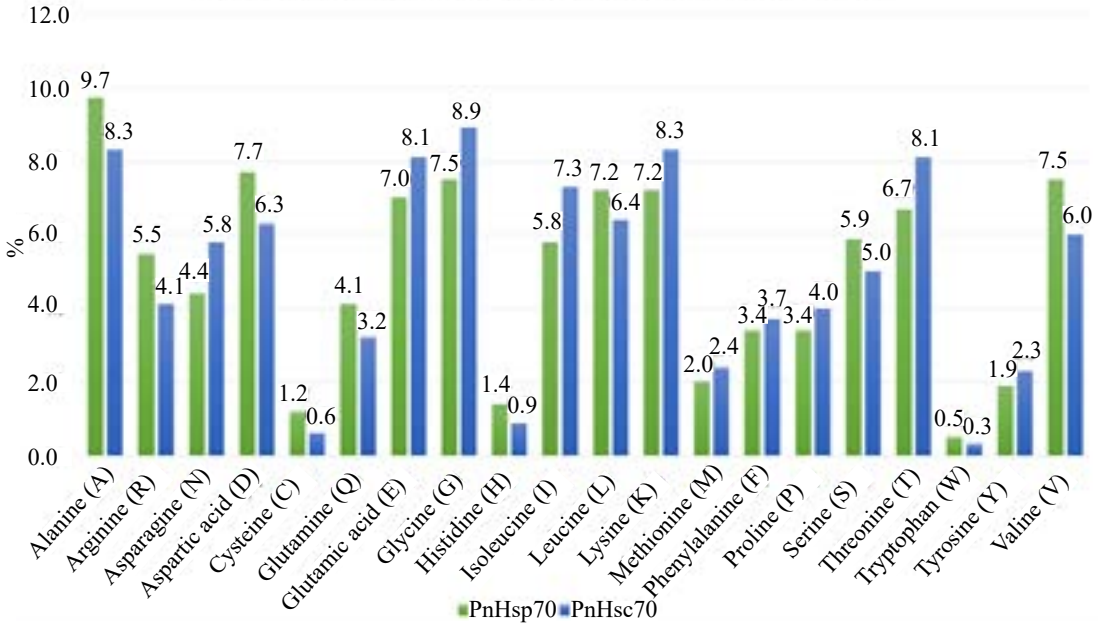

Figure 1. Amino acid composition of PnHsp70 and PnHsc70 proteins.

Table 2. Cysteine residue distribution and predicted disulfide bond pairing probabilities in PnHsp70 and PnHsc70 proteins

Protein	Position	Status	Score
PnHsp70	Cys17	no SS-bond	-50.1
	Cys98	no SS-bond	-26.5
	Cys307	no SS-bond	-20.5
	Cys356	no SS-bond	-16.1
	Cys372	no SS-bond	-24.4
	Cys423	probably no SS-bond	-6.8
	Cys573	probably no SS-bond	-4.1
	Cys602	no SS-bond	-6.8
PnHsc70	Cys18	no SS-bond	-57.4
	Cys268	no SS-bond	-33.4
	Cys547	no SS-bond	-20.6
	Cys604	no SS-bond	-27.2

in both proteins; (2) IFDLGGGTFDVSVL in PnHsp70 and IFDLGGGTFDVSIL in PnHsc70; and (3) VVLVGGSTRIPKIQS in PnHsp70 and IVLVGGSTRIPKVQK in PnHsc70 (Gupta & Singh, 1994). In addition, both proteins contained the conserved EEVD motif at the C-terminus, which is characteristic of cytosolic Hsp70 family proteins.

Three-dimensional molecular structures of PnHsp70 and PnHsc70 were predicted using the I-TASSER web server (https://zhanglab.ccmb.med.umich.edu/I-TASSER/). This platform generates protein structural models based on homologous templates available in the Protein Data Bank (PDB) (https://www.rcsb.org/) (Yang & Zhang, 2015). The five closest structural analogs for PnHsp70 and PnHsc70 are listed in Table 3. The top PDB hit for PnHsp70 was Hsp70 from *Chaetomium thermophilum* var. *thermophilum* DSM 1495 (PDB ID: 5tkyA), with a TM-score of 0.922, whereas PnHsc70 showed the highest similarity to Hsp70 from *Homo sapiens* (PDB ID: 5e84A), with a TM-score of 0.919. Since TM-scores above 0.5 indicate similar protein folds, both PnHsp70 and PnHsc70 are predicted to possess conserved tertiary structures comparable to those of Hsp70 proteins from *C. thermophilum, Homo sapiens, Saccharomyces cerevisiae*, and *Rattus norvegicus*.

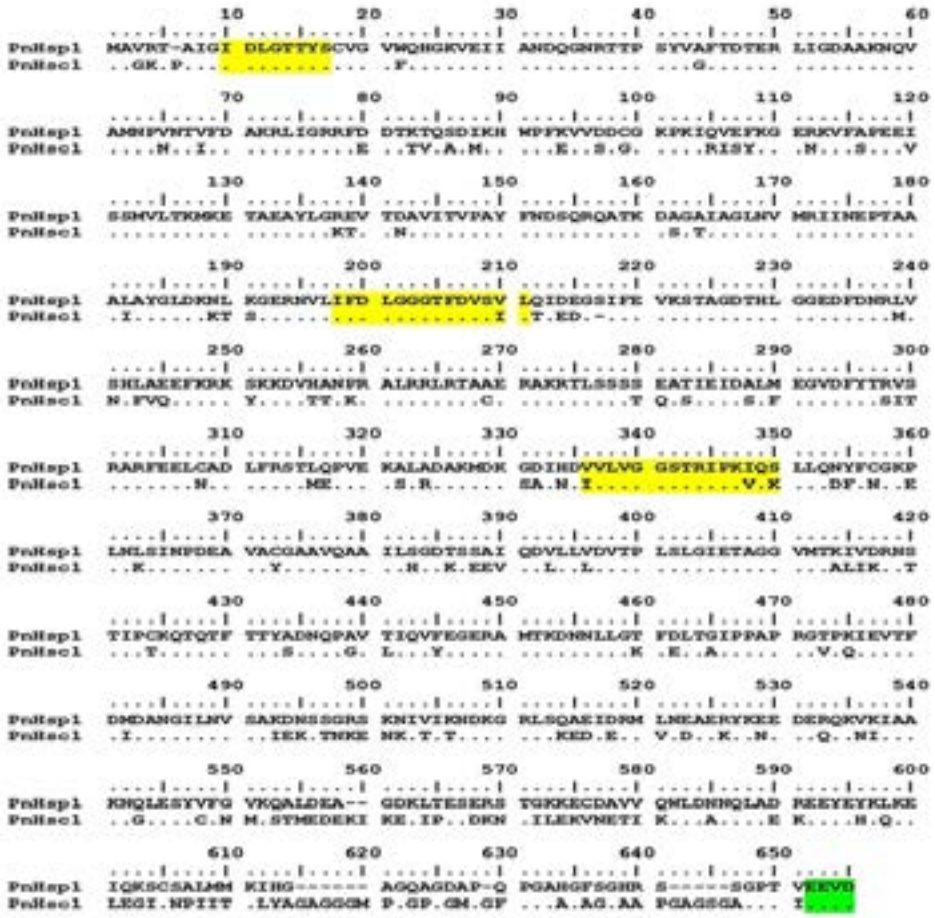

Figure 2. Multiple sequence alignment of PnHsp70 and PnHsc70 amino acid sequences showing three conserved Hsp70 signature motifs (highlighted in yellow) and the EEVD motif at the C-terminus (highlighted in green). Dots indicate conserved amino acid residues between the aligned sequences.

Table 3. Top structural analogs of PnHsp70 and PnHsc70 identified from the Protein Data Bank (PDB) based on I-TASSER analysis

	PDB ID	Protein	Species	TM-score	RMSD[a]	IDEN[a]	Cov.
PnHsp70	5tkyA	Hsp70	*Chaetomium thermophilum* var. *thermophilum* DSM 1495	0.922	0.900	0.559	0.931
	5e84A	Hsp70	*Homo sapiens*	0.898	1.990	0.587	0.934
	3d2fA	Hsp70	*Saccharomyces cerevisiae*, *Homo sapiens*	0.802	4.360	0.269	0.931
	6gfaA	HSP110	*Homo sapiens*	0.570	1.180	0.391	0.580
	4j8fA	Hsp70	*Homo sapiens, Rattus norvegicus*	0.561	3.480	0.620	0.628
PnHsc70	5e84A	Hsp70	*Homo sapiens*	0.919	0.490	0.640	0.922
	5tkyA	Hsp70	*Chaetomium thermophilum* var. *thermophilum* DSM 1495	0.864	2.250	0.659	0.907
	3d2fA	Hsp70	*Saccharomyces cerevisiae, Homo sapiens*	0.812	3.970	0.260	0.928
	6gfaA	HSP110	*Homo sapiens*	0.556	1.290	0.383	0.567
	4j8fA	Hsp70	*Homo sapiens, Rattus norvegicus*	0.549	3.400	0.641	0.612

Although the TM-scores for PnHsp70 and PnHsc70 were highly similar, RMSD, sequence identity (IDEN), and coverage values differed, indicating that their tertiary structures are more conserved than their

primary or secondary structures. Comparisons between query proteins and their templates demonstrated that the templates generally contained shorter amino acid sequences than the predicted proteins (Figure 3).

The predicted secondary structures of PnHsp70 and PnHsc70 consisted primarily of α-helices, β-sheets, and coils. Structural analyses further indicated that both proteins possessed a conserved nucleotide-binding domain (NBD) at the N-terminus and a substrate-binding domain (SBD) at the C-terminus (Figure 4). The SBD was subdivided into SBDβ, composed of antiparallel β-sheets, and SBDα, composed mainly of α-helices. The NBD consisted of four domains forming two lobes, between which the ATP-binding region is located. Within the SBD, substrate polypeptides bind between the lobes of SBDβ, whereas SBDα functions as a lid covering the substrate-binding region (Zhu et al., 1996; Bukau & Horwich, 1998; Yang & Zhang, 2015; Gumiero et al., 2016).

Functional prediction analysis using I-TASSER indicated high confidence scores (C-scores) for both PnHsp70 and PnHsc70, with values of 0.85 and 0.87, respectively, based on PDB ID 3kvgA. The C-score ranges from 0 to 1, with higher values indicating greater confidence in the predicted model (Table 4). Both proteins were predicted to interact with ANP

Figure 3. Comparison of the predicted secondary structures of PnHsp70 and PnHsc70 with their closest structural homologs. A.PnHsp70 (green) compared with Hsp70 from *Chaetomium thermophilum* var. *thermophilum* DSM 1495 (PDB ID: 5TKY; purple); B. PnHsc70 (green) compared with Hsp70 from Homo sapiens (PDB ID: 5E84; purple).

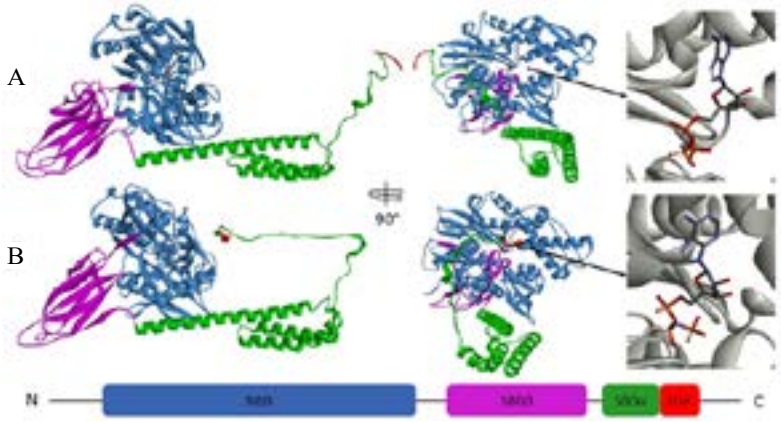

Figure 4. Predicted domain organization and structural architecture of PnHsp70 (A, B) and PnHsc70 (C, D). Both proteins consist of an N-terminal nucleotide-binding domain (NBD; blue) and a C-terminal substrate-binding domain (SBD), which is subdivided into SBDβ (purple), composed of antiparallel β-sheets, and SBDα (green), composed of α-helices. The conserved EEVD motif is located at the C-terminus (red). Ligand-binding sites are located within the NBD, between its four subdomains (lobes).

Table 4. Predicted residue-specific ligand-binding probabilities for PnHsp70 and PnHsc70 proteins

	PDB ID	C-score	Clust. size	Ligand	Ligand-binding sites residues
PnHsp70	3kvgA	0.85	144	ANP	12,13,14,15,201,202,203,204,231,269,272,273,276,339, 340,341,343,344,367
	2bupA	0.10	23	PO4	12,13,71,147,175,230
PnHsc70	3kvgA	0.87	130	ANP	13,14,15,16,202,203,204,205,231,269,272,273,276,339, 340,341,343,344,367
	1s3xA	0.10	23	PO4	13,14,72,148,176,230

(phosphoaminophosphonic acid–adenylate ester) ligands. In addition, phosphate ion (PO4) binding sites were detected in both proteins, although these predictions were associated with relatively low C-scores (0.10).

Besides ligand prediction, I-TASSER analysis also identified potential Enzyme Commission (EC) numbers and active sites. Both PnHsp70 and PnHsc70 were predicted to possess active sites capable of binding substrates such as hexokinase, glucokinase, and deoxyribonuclease I (Table 5). Similar substrate-binding predictions have previously been reported for Hsp70 and Hsc70 proteins in *Megalobrama amblycephala* (Tran et al., 2015).

Phylogenetic analysis based on amino acid sequences (Figure 5A–B) showed that PnHsp70

Table 5. Predicted Enzyme Commission (EC) numbers and active sites of PnHsp70 and PnHsc70 proteins

	Csc^{EC}	PDB ID	TM-sc	RMSD[a]	IDEN[a]	Cov	EC No.	EC name
PnHsp70	0.249	1qhaA	0.394	5.09	0.077	0.491	2.7.1.1	Hexokinase
	0.245	3hm8A	0.382	4.33	0.109	0.459	2.7.1.1	Hexokinase
	0.241	3f9mA	0.387	4.22	0.103	0.461	2.7.1.2	Glucokinase
	0.192	3cjcA	0.419	4.00	0.156	0.489	3.1.21.1	Deoxyribonuclease I
PnHsc70	0.184	1hkgA	0.384	4.93	0.087	0.475	2.7.1.1	Hexokinase
	0.259	1qhaA	0.387	5.12	0.084	0.483	2.7.1.1	Hexokinase
	0.259	3cjcA	0.410	4.10	0.137	0.480	3.1.21.1	Deoxyribonuclease I
	0.258	3f9mA	0.375	4.08	0.108	0.442	2.7.1.2	Glucokinase
	0.246	3hm8A	0.372	4.39	0.110	0.448	2.7.1.1	Hexokinase
	0.202	1v4tA	0.278	4.90	0.056	0.341	2.7.1.2 2.7.1.1	Glucokinase Hexokinase

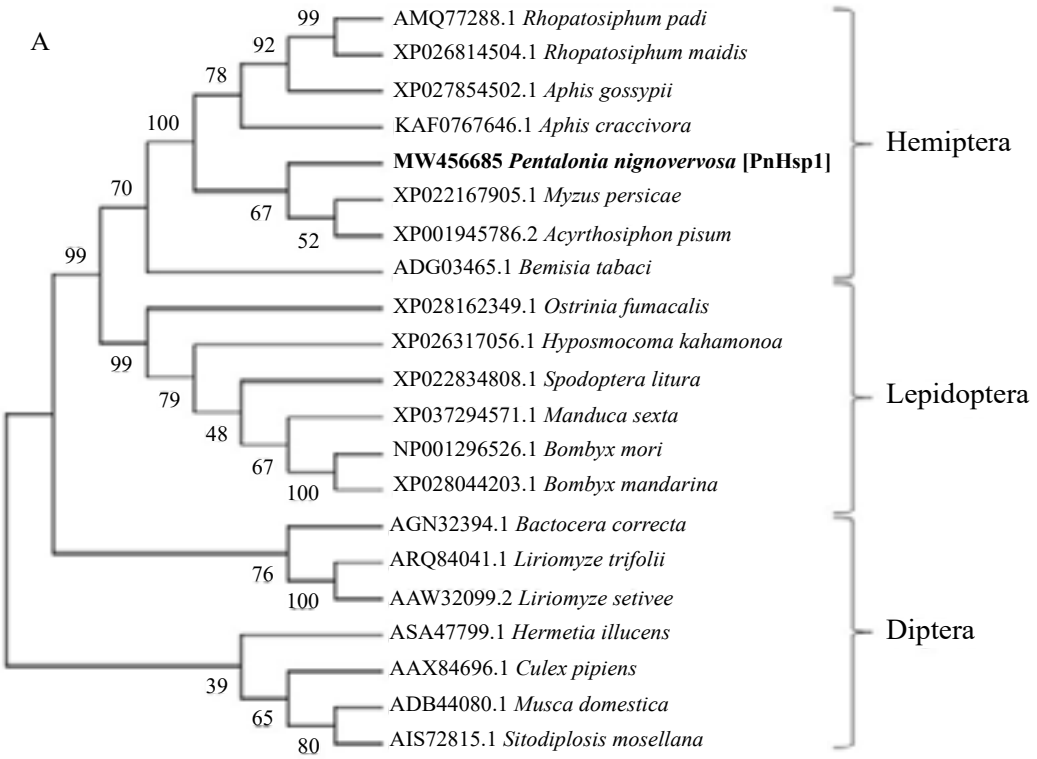

Figure 5. Phylogenetic analysis of PnHsp70 and PnHsc70 proteins. A. Neighbor-joining (NJ) phylogenetic tree of PnHsp70 and homologous Hsp70 proteins from insect species belonging to the orders Hemiptera, Lepidoptera, and Diptera; B. Neighbor-joining (NJ) phylogenetic tree of PnHsc70 and homologous Hsc70 proteins from insect species belonging to the orders Hemiptera, Lepidoptera, and Diptera. Trees were constructed using amino acid sequences with the Poisson correction model, pairwise deletion, and 1000 bootstrap replications. Bootstrap support values (%) are shown at the nodes.

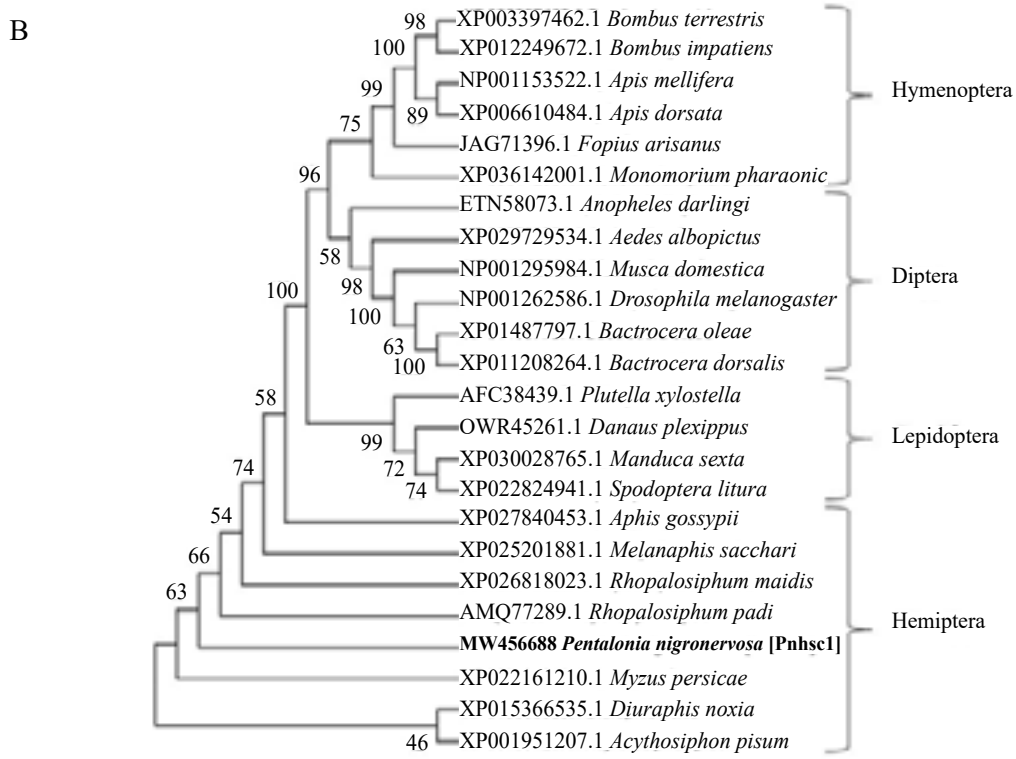

Figure 5. Continued. Phylogenetic analysis of PnHsp70 and PnHsc70 proteins. A. Neighbor-joining (NJ) phylogenetic tree of PnHsp70 and homologous Hsp70 proteins from insect species belonging to the orders Hemiptera, Lepidoptera, and Diptera; B. Neighbor-joining (NJ) phylogenetic tree of PnHsc70 and homologous Hsc70 proteins from insect species belonging to the orders Hemiptera, Lepidoptera, and Diptera. Trees were constructed using amino acid sequences with the Poisson correction model, pairwise deletion, and 1000 bootstrap replications. Bootstrap support values (%) are shown at the nodes.

(PnHsp1) clustered with Hsp70 homologs from other hemipteran species, particularly *Myzus persicae* and *Acyrthosiphon pisum*. Across insect orders, PnHsp70 also grouped within a broader clade containing several lepidopteran Hsp70 proteins, reflecting conserved evolutionary relationships. In contrast, PnHsc70 (PnHsc1) formed a distinct branch separated from Hsc70 orthologs of Hymenoptera, Diptera, and Lepidoptera, indicating a more divergent evolutionary trajectory.

Differentially Expressed Genes (DEGs) and qRT-PCR Validation of PnHSP70 and PnHsc70. The analysis of differentially expressed genes (DEGs) between BBTV-viruliferous (BBTV-Vr) and BBTV-non-viruliferous (BBTV-NVr) *P. nigronervosa* is presented in Figure 6. The results showed that the expression of PnHsp1, PnHsp2, and PnHsc1 was influenced by BBTV acquisition in *P. nigronervosa.*

To validate these findings, *P. nigronervosa* individuals were exposed to BBTV-infected banana plants for different plant access periods (PAPs; 0, 1, 5, 10, and 20 hours) (Figure 7). When *P. nigronervosa* had no access to BBTV-infected banana plants (0 hour PAP), the mean fold change of PnHsp70 expression was 1.05. After 1 hour of feeding on BBTV-infected banana plants, PnHsp70 expression increased markedly to 3.96-fold, followed by slight decreases at 5 hours (3.65-fold) and 10 hours (0.93-fold). However, expression increased again to 3.93-fold at 20 hours PAP. Although statistical differences among PAP treatments were not significant, the overall trend indicated upregulation of PnHsp70 expression in response to prolonged feeding on BBTV-infected banana plants.

Functional validation of PnHsp70 was demonstrated through its differential expression following BBTV acquisition during feeding by *P. nigronervosa.* PnHsp70 exhibited dynamic transcriptional changes across PAP treatments, with overall upregulation dominating the response pattern. Viral entry, including that of BBTV, generally begins with interactions between viral proteins and receptors on the vector cell surface. Such interactions can activate stress-responsive signaling pathways, including Hsp70

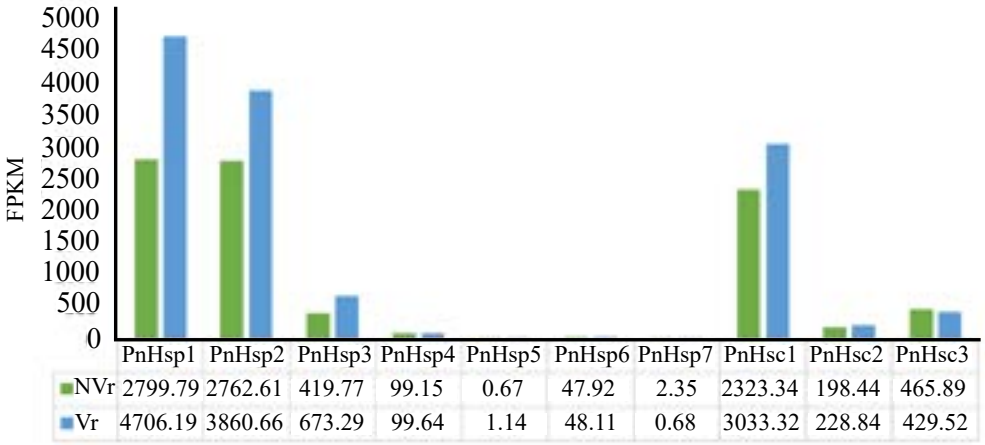

	PnHsp1	PnHsp2	PnHsp3	PnHsp4	PnHsp5	PnHsp6	PnHsp7	PnHsc1	PnHsc2	PnHsc3
NVr	2799.79	2762.61	419.77	99.15	0.67	47.92	2.35	2323.34	198.44	465.89
Vr	4706.19	3860.66	673.29	99.64	1.14	48.11	0.68	3033.32	228.84	429.52

Figure 6. FPKM-based expression levels of PnHsp1–PnHsp7 and PnHsc1–PnHsc3 in BBTV-viruliferous (Vr) and non-viruliferous (NVr) *Pentalonia nigronervosa*, as determined by differential gene expression (DEG) analysis of RNA-seq datasets (GenBank accessions SRX6918251 and SRX6918252).

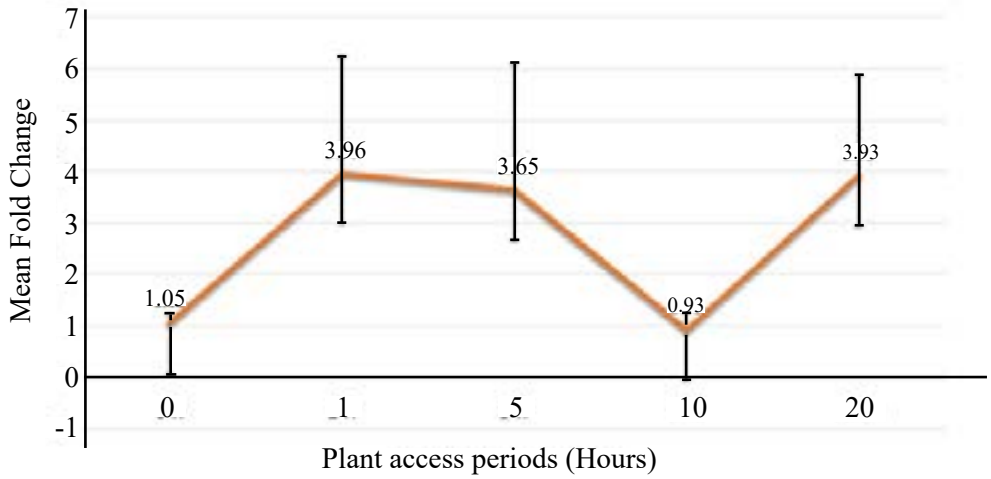

Figure 7. Relative expression (fold change) of the PnHsp70 gene in *Pentalonia nigronervosa* after different plant access periods (PAPs; 0, 1, 5, 10, and 20 hours) on BBTV-infected banana plants. Expression levels were determined by qRT-PCR and normalized against the actin reference gene using the 2^-ΔΔCt method.

induction. A similar mechanism has been described in the TYLCV–*Bemisia tabaci* interactions, in which Heat Shock Factor (HSF) translocates to the nucleus, binds heat shock elements (HSEs), and activates Hsp70 transcription (Sarge et al., 1993; Götz et al., 2012). These findings suggest that BBTV may similarly trigger PnHsp70 expression through analogous molecular pathways in *P. nigronervosa*.

The observed induction of PnHsp70 following BBTV exposure is consistent with the known role of Hsp70 as an inducible stress-responsive protein within the Hsp70 family (Whitley et al., 1999). PnHsp70 upregulation at the 20-hour PAP may reflect the movement of BBTV toward the anterior midgut (AMG), consistent with reports that Hsp70 expression is higher in insect fat bodies than in the AMG (Shu et al., 2011). Therefore, the fluctuating expression profile observed in this study may correspond to different stages of BBTV movement and interaction within vector tissues.

In addition to viral infection, environmental factors such as temperature and insect developmental stage may also influence Hsp70 expression (Anhalt & Almeida, 2008). Nevertheless, the BBTV-induced upregulation of PnHsp70 strongly suggests its functional involvement in BBTV acquisition, persistence, or transmission. Similar findings have been reported in TYLCV, where interference with Hsp70 altered viral transmission efficiency in *B. tabac*i (Götz et al., 2012). These observations support the hypothesis that viruses may exploit host Hsp70 machinery to facilitate intracellular movement, protein stabilization, or protection against host defenses within the vector.

The dual role of Hsp70 as both a cytoprotective chaperone and a facilitator of pathogenic processes has also been reported in other biological systems, including cancer biology (Vostakolaei et al., 2021). Therefore, understanding the mechanistic role of PnHsp70 in BBTV acquisition and transmission provides valuable insights into vector–virus molecular interactions and may contribute to the development of innovative BBTV management strategies aimed at disrupting viral transmission in a sustainable manner.

CONCLUSION

This study provides the first comprehensive characterization of the Hsp70 and Hsc70 gene families in *Pentalonia nigronervosa* and demonstrates that several members, particularly PnHsp1, PnHsp2, and PnHsc1, respond to BBTV acquisition. Structural and functional analyses confirmed that these proteins possess conserved Hsp70-family characteristics, whereas differential gene expression analysis and plant access period assays revealed dynamic transcriptional regulation associated with BBTV exposure. The observed upregulation of PnHsp70 suggests a potential role in the intracellular trafficking, maintenance, and transmission of BBTV within *P. nigronervosa.* Collectively, these findings provide new insights into the molecular interactions between BBTV and its aphid vector and highlight Hsp70 as a promising target for developing innovative strategies to interfere with BBTV transmission and improve the management of banana bunchy top disease.

ACKNOWLEDGMENTS

The authors gratefully acknowledge the laboratory support provided by the Genetic Engineering Laboratory and the Molecular Entomology Laboratory, Department of Plant Protection, Faculty of Agriculture, Universitas Gadjah Mada.

FUNDING

This research was supported by the Bill & Melinda Gates Foundation under Grant No. OPP1130226 and by the Master's Research Scheme Program of the Ministry of Research and Technology/ National Research and Innovation Agency of the Republic of Indonesia under Grant No. 3048/UN1. DITLIT/DIT-LIT/PT/2020.

AUTHORS' CONTRIBUTIONS

IN performed the experiments, analyzed the data, and drafted the manuscript. AS contributed to the conceptualization, methodology, validation, and revision of the manuscript. SS contributed to the conceptualization, funding acquisition, supervision, and revision of the manuscript. All authors read and approved the final manuscript.

COMPETING INTEREST

The authors declare that they have no competing interests.

REFERENCES

Alam SB & Rochon DA. 2015. Cucumber necrosis virus recruits cellular heat shock protein 70 homologs at several stages of infection. *J. Virol*. 90(7): 3302–3317. https://doi.org/10.1128/JVI.02833-15

Anhalt MD & Almeida RPP. 2008. Effect of temperature, vector life stage, and plant access period on transmission of banana bunchy top virus to banana. *Phytopathol*. 98(6): 743–748. https://doi.org/10.1094/PHYTO-98-6-0743

Arimbawa IM, Wirya GNAS, & Sudiarta IP. 2022. First report of Banana bunchy top virus on heliconia (*Heliconia* spp.) in Bali, Indonesia. *J. Trop. Plant Pests Dis.* 22(1): 77–82. https://doi.org/10.23960/jhptt.12277-82

Arsi, Suparman, Pujiastuti Y, & Irsan C. 2025. Epidemiology of banana bunchy top disease in South Sumatra, Indonesia. *J. Trop. Plant Pests Dis.* 25(2): 298–308. https://doi.org/10.23960/jhptt.225298-308

Bukau B & Horwich AL. 1998. The Hsp70 and Hsp60 chaperone machines. *Cell*. 92(3): P351–366. https://doi.org/10.1016/S0092-8674(00)80928-9

Chang KY & Yang JR. 2013. Analysis and prediction of highly effective antiviral peptides based on random forests. *PLoS One*. 8(8): e70166. https://doi.org/10.1371/journal.pone.0070166

Folmer O, Black M, Hoeh W, Lutz R, & Vrijenhoek R. 1994. DNA primers for amplification of

mitochondrial cytochrome c oxidase subunit I from diverse metazoan invertebrates. *Mol. Mar. Biol. Biotechnol*. 3(5): 294–299. https://pubmed.ncbi.nlm.nih.gov/7881515/

Gorovits R, Moshe A, Ghanim M, & Czosnek H. 2013. Recruitment of the host plant heat shock protein 70 by tomato yellow leaf curl virus coat protein is required for virus infection. *PLoS One*. 8(7): e70280. https://doi.org/10.1371/journal.pone.0070280

Götz M, Popovski S, Kollenberg M, Gorovits R, Brown JK, Cicero JM, Czosnek H, Winter S, & Ghanim M. 2012. Implication of *Bemisia tabaci* heat shock protein 70 in begomovirus-whitefly interactions. *J. Virol.* 86(24): 13241–13252. https://doi.org/10.1128/JVI.00880-12

Gumiero A, Conz C, Gesé GV, Zhang Y, Weyer FA, Lapouge K, Kappes J, von Plehwe U, Schermann G, Fitzke E, Wölfle T, Fischer T, Rospert S, & Sinning I. 2016. Interaction of the cotranslational Hsp70 Ssb with ribosomal proteins and rRNA depends on its lid domain. *Nat. Commun.* 7(1): 13563. https://doi.org/10.1038/ncomms13563

Gupta RS & Singh B. 1994. Phylogenetic analysis of 70 kD heat shock protein sequences suggests a chimeric origin for the eukaryotic cell nucleus. *Curr. Biol.* 4(12): 1104–1114. https://doi.org/10.1016/S0960-9822(00)00249-9

Guruprasad K, Reddy BVB, & Pandit MW. 1990. Correlation between stability of a protein and its dipeptide composition: a novel approach for predicting in vivo stability of a protein from its primary sequence. *Protein Eng. Des. Sel.* 4(2): 155–161. https://doi.org/10.1093/protein/4.2.155

Hall TA. 1999. BioEdit: A user-friendly biological sequence alignment editor and analysis program for Windows 95/98/NT. *Nucl. Acids Symp. Ser.* 41: 95–98. https://doi.org/10.14601/Phytopathol_Mediterr-14998u1.29

Hartl FU, Bracher A, & Hayer-Hartl M. 2011. Molecular chaperones in protein folding and proteostasis. *Nature*. 475(7356): 324–332. https://doi.org/10.1038/nature10317

Hu C, Yang J, Qi Z, Wu H, Wang B, Zou F, Mei H, Liu J, Wang W, & Liu Q. 2022. Heat shock proteins: Biological functions, pathological roles, and therapeutic opportunities. *MedComm*. 3(3): e161. https://doi.org/10.1002/mco2.161

Ikai A. 1980. Thermostability and aliphatic index of globular proteins. *J. Biochem.* 88(6): 1895–1898. https://doi.org/10.1093/oxfordjournals.jbchem.a133168

Jiang S, Lu Y, Li K, Lin L, Zheng H, Yan F, & Chen J. 2014. Heat shock protein 70 is necessary for rice stripe virus infection in plants. *Mol. Plant Pathol.* 15(9): 907–917. https://doi.org/10.1111/mpp.12153

Kampinga HH, Hageman J, Vos MJ, Kubota H, Tanguay RM, Bruford EA, Cheetham ME, Chen B, & Hightower LE. 2009. Guidelines for the nomenclature of the human heat shock proteins. *Cell Stress Chap*. 14(1): 105–111. https://doi.org/10.1007/s12192-008-0068-7

Kregel KC. 2002. Invited Review: Heat shock proteins: modifying factors in physiological stress responses and acquired thermotolerance. *J. Appl. Physiol.* 92(5): 2177–2186. https://doi.org/10.1152/japplphysiol.01267.2001

Kyte J & Doolittle RF. 1982. A simple method for displaying the hydropathic character of a protein. *J. Mol. Biol*. 157(1): 105–132. https://doi.org/10.1016/0022-2836(82)90515-0

Lang BJ, Guerrero ME, Prince TL, Okusha Y, Bonorino C, & Calderwood SK. 2021. The functions and regulation of heat shock proteins: Key orchestrators of proteostasis and the heat shock response. *Arch. Toxicol.* 95(6): 1943–1970. https://doi.org/10.1007/s00204-021-03070-8

Livak KJ & Schmittgen TD. 2001. Analysis of relative gene expression data using real-time quantitative PCR and the $2^{-\Delta\Delta CT}$ method. *Methods*. 25(4): 402–408. https://doi.org/10.1006/meth.2001.1262

Nakamoto H, Fujita K, Ohtaki A, Watanabe S, Narumi S, Maruyama T, Suenaga E, Misono TS, Kumar PKR, Goloubinoff P, & Yoshikawa H. 2014. Physical interaction between bacterial heat shock protein 90 and Hsp70 chaperones mediates their cooperative action to refold denatured proteins. *J. Biol. Chem.* 289(9): P6110–6119. https://doi.org/10.1074/jbc.M113.524801

Pusag JCA, Jahan SH, Lee KS, Lee S, & Lee KY. 2012. Upregulation of temperature susceptibility in *Bemisia tabaci* upon acquisition of tomato yellow leaf curl virus (TYLCV). *J. Insect Physiol.* 58(10): 1343–1348. https://doi.

org/10.1016/j.jinsphys.2012.07.008

Qazi J. 2016. Banana bunchy top virus and the bunchy top disease. *J. Gen. Plant Pathol.* 82(1): 2–11. https://doi.org/10.1007/s10327-015-0637-0

Sarge KD, Murphy SP, & Morimoto RI. 1993. Activation of heat shock gene transcription by heat shock factor 1 involves oligomerization, acquisition of DNA-binding activity, and nuclear localization and can occur in the absence of stress. *Mol. Cell. Biol*. 13(3): 1392–1407. https://doi.org/10.1128/mcb.13.3.1392-1407.1993

Shu Y, Du Y, & Wang J. 2011. Molecular characterization and expression patterns of *Spodoptera litura* heat shock protein 70/90, and their response to zinc stress. *Comp. Biochem. Physiol. Part A. Mol. Integ. Physiol.* 158(1): 102–110. https://doi.org/10.1016/j.cbpa.2010.09.006

Stainton D, Kraberger S, Walters M, Wiltshire EJ, Rosario K, Halafihi M, Lolohea S, Katoa I, Faitua TH, Aholelei W, Taufa L, Thomas JE, Collings DA, Martin DP, & Varsani1 A. 2012. Evidence of inter-component recombination, intra-component recombination and reassortment in banana bunchy top virus. *J. Gen. Virol.* 93(5): 1103–1119. https://doi.org/10.1099/vir.0.040337-0

Subandiyah S, Rahayuniati RF, Hartono S, Somowiyarjo S, & Soffan A. 2020. RNA-seq data of banana bunchy top virus (BBTV) viruliferous and non-viruliferous banana aphid (*Pentalonia nigronervosa*). *Data Br.* 28: 104860. https://doi.org/10.1016/j.dib.2019.104860

Taguwa S, Maringer K, Li X, Bernal-Rubio D, Rauch JN, Gestwicki JE, Andino R, Fernandez-Sesma A, & Frydman J. 2015. Defining Hsp70 subnetworks in dengue virus replication reveals key vulnerability in flavivirus infection. *Cell*. 163(5): P1108–1123. https://doi.org/10.1016/j.cell.2015.10.046

Tamura K, Stecher G, Peterson D, Filipski A, & Kumar S. 2013. MEGA6: Molecular Evolutionary Genetics Analysis Version 6.0. *Mol. Biol. Evol.* 30(12): 2725–2729. https://doi.org/10.1093/molbev/mst197

Thompson JD, Gibson TJ, Plewniak F, Jeanmougin F, & Higgins DG. 1997. The CLUSTAL_X windows interface: Flexible strategies for multiple sequence alignment aided by quality analysis tools. *Nucleic. Acids Res*. 25(24): 4876–4882. https://doi.org/10.1093/nar/25.24.4876

Tower J. 2011. Heat shock proteins and *Drosophila* aging. *Exp. Gerontol*. 46(5): 355–362. https://doi.org/10.1016/j.exger.2010.09.002

Tran NT, Jakovlić I, & Wang WM. 2015. In silico characterisation, homology modelling and structure-based functional annotation of blunt snout bream (*Megalobrama amblycephala*) Hsp70 and Hsc70 proteins. *J. Anim. Sci. Technol*. 57(1): 44. https://doi.org/10.1186/s40781-015-0077-x

Vostakolaei MA, Hatami-Baroogh L, Babaei G, Molavi O, Kordi S, & Abdolalizadeh J. 2021. Hsp70 in cancer: A double agent in the battle between survival and death. *J. Cell. Physiol*. 236(5): 3420–3444. https://doi.org/10.1002/jcp.30132

Wang XR, Wang C, Ban FX, Zhu DT, Liu SS, & Wang XW. 2019. Genome-wide identification and characterization of *HSP* gene superfamily in whitefly (*Bemisia tabaci*) and expression profiling analysis under temperature stress. *Insect Sci.* 26(1): 44–57. https://doi.org/10.1111/1744-7917.12505

Weeks SA, Shield WP, Sahi C, Craig EA, Rospert S, & Miller DJ. 2010. A targeted analysis of cellular chaperones reveals contrasting roles for heat shock protein 70 in flock house virus RNA replication. *J. Virol.* 84(1): 330–339. https://doi.org/10.1128/jvi.01808-09

Whitley D, Goldberg SP, & Jordan WD. 1999. Heat shock proteins: A review of the molecular chaperones. *J. Vasc. Surg.* 29(4): 748–751. https://doi.org/10.1016/S0741-5214(99)70329-0

Wiedemann C, Kumar A, Lang A, & Ohlenschläger O. 2020. Cysteines and disulfide bonds as structure-forming units: Insights from different domains of life and the potential for characterization by NMR. *Front. Chem*. 8: 280. https://doi.org/10.3389/fchem.2020.00280

Yang J & Zhang Y. 2015. I-TASSER server: New development for protein structure and function predictions. *Nucleic Acids Res.* 43(W1): W174–

W181. https://doi.org/10.1093/nar/gkv342

Zhu X, Zhao X, Burkholder WF, Gragerov A, Ogata CM, Gottesman ME, & Hendrickson WA. 1996. Structural analysis of substrate binding by the molecular chaperone DnaK. *Science*. 272(5268): 1606–1614. https://doi.org/10.1126/science.272.5268.1606